
No Supermassive Black Hole in M33?¹

David Merritt, Laura Ferrarese, Charles L. Joseph

Department of Physics and Astronomy, Rutgers University, New Brunswick, NJ 08854

We observed the nucleus of M33, the third-brightest galaxy in the Local Group, with the Space Telescope Imaging Spectrograph at a resolution at least a factor of 10 higher than previously obtained. Rather than the steep rise expected within the radius of gravitational influence of a supermassive black hole, the random stellar velocities showed a decrease within a parsec of the center of the galaxy. The implied upper limit on the mass of the central black hole is only $3000M_{\odot}$, about three orders of magnitude lower than the dynamically-inferred mass of any other supermassive black hole. Detecting black holes of only a few thousand solar masses is observationally challenging but is critical for establishing how supermassive black holes relate to their host galaxies and which mechanisms influence the formation and evolution of both.

At a distance of 850 kpc from Earth, M33 is classified (1) as a late-type ScII-III spiral, consistent with its almost nonexistent bulge (2,3). The nucleus of M33 is very compact, reaching a stellar central mass density of several million solar masses per cubic parsec (4,5), larger than that of any globular cluster. While such high nuclear densities might be expected in the presence of a supermassive black hole (SMBH) (6), ground-based data show no evidence for a central rise in stellar velocities that would indicate the presence of a compact massive object in the nucleus (4).

M33 was observed on 12 February 1999 with the Space Telescope Imaging Spectrograph (STIS) on the Hubble Space Telescope (HST). Three sets of two long-slit spectra each, for a total exposure time of 7380 seconds, were obtained using the G750M grating centered on the CaII absorption triplet near 8561 Å (1 Å corresponds to 10^{-10} meters), covering $19.6 \text{ km s}^{-1} \text{ pixel}^{-1}$. The pixel scale is $0''.05$ with a spatial resolution of $0''.115$ at 8561 Å. While the two spectra in each set were obtained at the same position to facilitate removal of cosmic ray events, the nucleus was moved along the slit by $0''.216$ between each consecutive set. This dithering procedure allows for optimal correction of residual

¹Submitted to **Science** 27 June 2001; accepted 12 July 2001; published 19 July 2001. Online version at **Science Express** (www.sciencexpress.org). Print version appears in the 10 August 2001 issue of **Science**.

variations in the detector sensitivity as well as identification and removal of malfunctioning pixels. The calibration steps followed the standard procedure (7) adopted for STIS observations of the nucleus of M32.

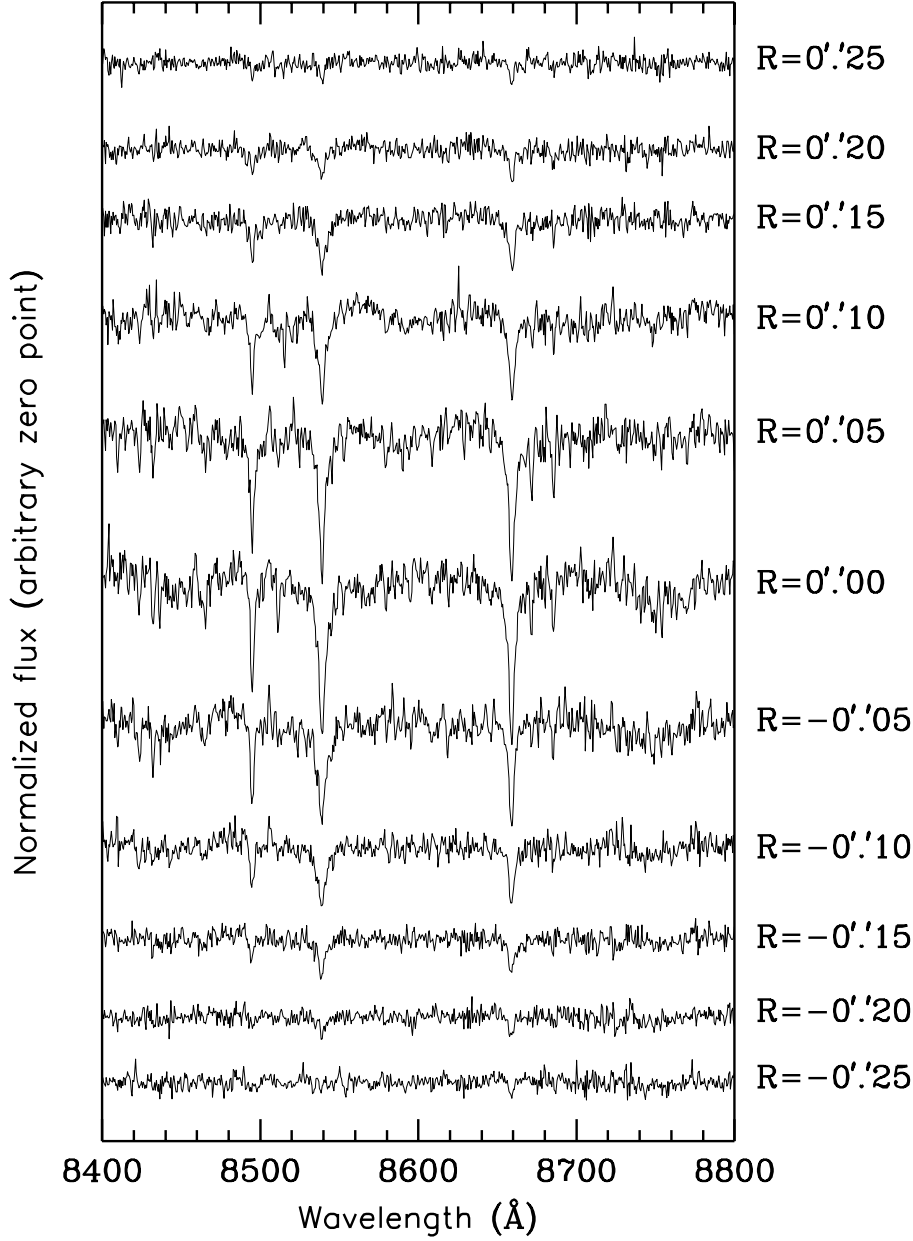


Figure 1. HST/STIS spectra of M33 extracted at the location of the nucleus of the galaxy (central row, marked $R = 0''.00$) and up to $0''.25$ (1.0 pc) off-nucleus. The spectra have been shifted by an arbitrary amount in the vertical direction but the same scale has been maintained. The decrease in the velocity dispersion of the CaII absorption lines (8561 Å) at the central positions is visible.

The observed spectrum (Fig. 1) at every resolution element is the convolution of the spectra of individual stars with the line-of-sight velocity distribution (LOSVD) of the stellar ensemble; the latter contains information about the mean and random velocities of stars in the nucleus, projected along the line of sight through the galaxy. As a typical stellar spectrum we adopted that of the K0 III giant star HD7615 which was observed with the same instrumental configuration. LOSVDs were extracted from the STIS spectra using the Maximum Penalized Likelihood (MPL) algorithm (8) and represented in terms of Gauss-Hermite series (9) at every slit position. The mean velocity V_0 and velocity dispersion σ_0 are given (modulo a standard correction applied to V_0 (9)) by the first two terms in the Gauss-Hermite expansion.

Neither V_0 nor σ_0 show the rise that would be expected to occur whenever a black hole of mass M_\bullet significantly influences the motion of the stars, i.e. within a distance from the center of the galaxy

$$r_h \equiv \frac{GM_\bullet}{\sigma^2} \approx 0.028'' \left(\frac{M_\bullet}{10^4 M_\odot} \right) \left(\frac{\sigma}{20 \text{ km s}^{-1}} \right)^{-2} \quad (1)$$

as seen at the distance of M33. In particular, the central velocity dispersion is $24 \pm 3 \text{ km s}^{-1}$, significantly *lower* than the dispersion of $\sim 35 \pm 5 \text{ km s}^{-1}$ at $\pm 0.3'' \approx 1.2 \text{ pc}$. Given the $\sim 0.05''$ resolution of STIS, equation (1) implies $M_\bullet \lesssim 10^4 M_\odot$.

The predicted velocities, however, depend not only on M_\bullet , but also on the gravitational potential due to the stars and on the form of the stellar orbits around the putative black hole (for example are the stellar orbits eccentric or circular). Therefore, a more rigorous upper limit to the mass of a possible black hole can be derived by constructing realistic dynamical models of the M33 nucleus, which we assume to be spherical based on its projected circular shape (5). While a face-on disk would also project circular isophotes, the position angle and ellipticity of the nucleus and the outer disk are considerably different, implying that the former is unlikely to be a simple extension of the latter. Furthermore, the properties of the M33 nucleus are consistent with those observed for globular clusters (4) - the prototypical spherical systems. The luminosity density (2,5,10) was represented by

$$\nu(r) = \nu_0 \left(\frac{r}{a} \right)^{-\gamma} \left(1 + \frac{r}{a} \right)^{\gamma-4}. \quad (2)$$

In the above equation, a is the distance from the center of the galaxy at which the luminosity density is a fraction (in our case, one quarter) of the central value ν_0 , while γ defines the gradient in the luminosity density for $r \ll a$. We adopt $\gamma = 2$ and $a = 1 \text{ kpc}$ (5); ν_0 was fixed by requiring the luminosity within 1 pc of the center to be $1.0 \times 10^6 L_\odot$. The gravitational potential due to the stars was derived from $\nu(r)$ and from Poisson's equation as a function of the parameter M/L , the ratio of stellar mass to V -band luminosity expressed in solar units. Past studies found $M/L \lesssim 0.5$ suggestive of a young stellar population (4,11).

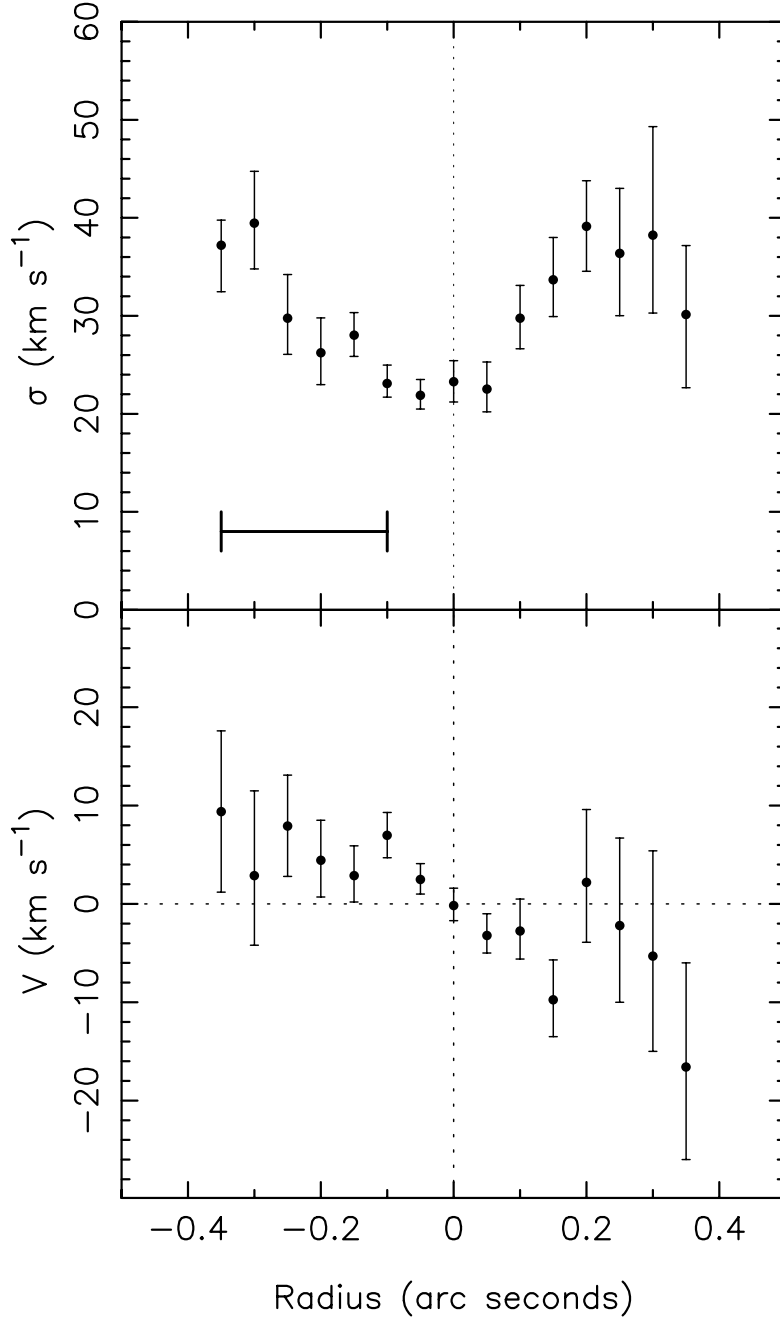


Figure 2. The stellar rotation curve (lower panel) and velocity dispersion profile (upper panel) of stars in the nucleus of M33, derived from the STIS spectra as described in the text. One-sigma error bars are shown. Also shown is the angular scale corresponding to 1 parsec at the distance of M33.

For a dynamically relaxed stellar system in a spherical gravitational potential, the number of stars which occupy a given location in velocity-position space, may be any non-negative function $f(E, l)$ of the orbital energy E and angular momentum l . We used standard techniques (12) to find the f which best reproduced the kinematical data given M_\bullet and M/L , subject to the constraint that the integral of f over velocities reproduced the assumed luminosity density $\nu(r)$. The velocities predicted by f were projected onto the plane of the sky and convolved with the HST point spread function (PSF) and the STIS slit in order to allow direct comparison with the observed velocities. We emphasize that a two-integral ($f(E, L)$) model for a spherical system, like the model adopted here, permits precisely as much flexibility in the orbital distribution as a three-integral model for an axisymmetric system. In other words, the constraints on the mass of the M33 SMBH derived from a three-integral modelling code would be precisely the same as those found here unless the underlying stellar potential were assumed to be significantly nonspherical.

In the absence of any additional constraints on f , we found that even black holes with $M_\bullet \gtrsim 50000 M_\odot$ could be made consistent with the data. However the f 's corresponding to these large values of M_\bullet were always found to be physically unreasonable: the stellar orbits changed suddenly from nearly circular at $r \gtrsim 0.1$ pc to nearly radial at $r \lesssim 0.1$ pc, causing the projected velocity dispersion to drop sharply at a radius corresponding to the angular size of the STIS PSF before rising again near the black hole. After convolution with the PSF, the observed velocities in these solutions therefore remained low even when M_\bullet was large. To avoid such unphysical behavior, the solutions for f were regularized (12), i.e. forced to be smooth; the regularization parameter was chosen to be just large enough to suppress unphysical features on the scale of the PSF.

Even after regularization, reasonable fits to the data with $M_\bullet \gtrsim 10000 M_\odot$ could still be found for values of the stellar mass to light ratio lower than $0.1 M_\odot/L_\odot$. This can be understood qualitatively as follows. The gravitational potential is defined by the joint contribution of the stars and the central black hole. Decreasing the stellar mass-to-light ratio has the effect of diminishing the stellar contribution to the central potential; to compensate, the mass of the black hole needs to be increased proportionally. Decreasing M/L also has the more subtle effect of requiring the stellar orbits to become predominantly radial at large distances. As a result, the predicted line-of-sight velocity dispersion drops suddenly just outside of the fitted region, contrary to what is observed: the velocity dispersion in the M33 bulge appears to remain high, $\sigma \approx 34 \text{ km s}^{-1}$, within $R \approx 80''$ (13). By forcing the rms line-of-sight velocity dispersion to be greater than 30 km s^{-1} in the radial range $0''.5 < R < 20''$, such unphysical solutions were excluded.

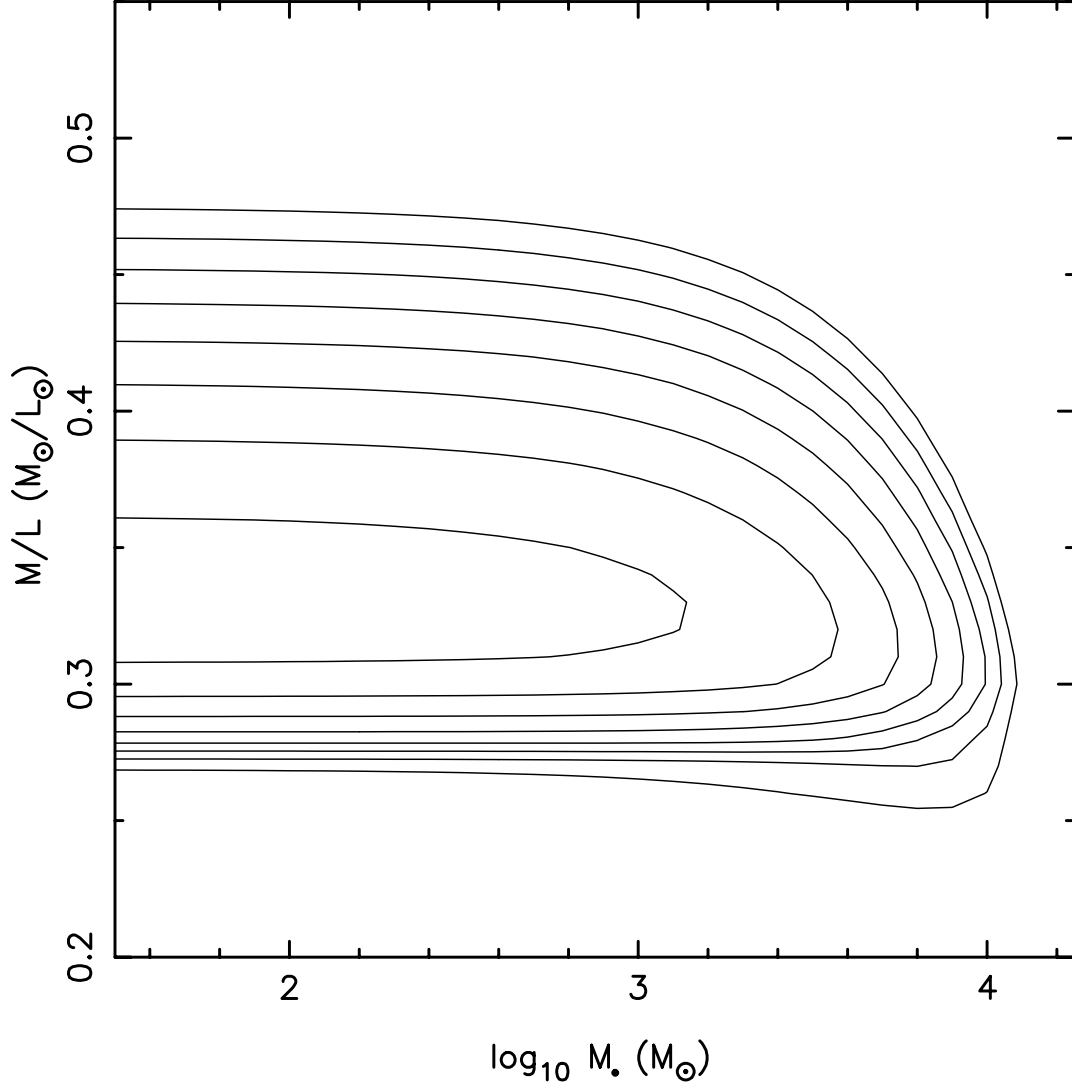


Figure 3. Contours of constant $\tilde{\chi}^2$ measuring the fit of the dynamical models described in the text to the data of Figure 2. Horizontal axis is the assumed mass of a central black hole and vertical axis is the mass-to-light ratio of the stars in the bulge. The lowest plotted contour is at $\tilde{\chi}^2 = 1.4$ and contours are separated by 0.2.

The best-fit f subject to these constraints was computed over a grid of $(M_\bullet, M/L)$ values (Fig. 3). For $M_\bullet \lesssim 1000M_\odot$ and $M/L \approx 0.35$, the mass of the putative black hole is too small to significantly affect the observable velocities and the quality of the fit is independent of M_\bullet . As M_\bullet is increased above $\sim 2000M_\odot$, $\tilde{\chi}^2$ increases as the rise in the central value of σ provides a progressively worse fit to the data at $R \lesssim 0''.1$. Values of M_\bullet as large as $\sim 3000M_\odot$ imply $\tilde{\chi}^2 \approx 1.7$ when only the data in the innermost two or three points are compared with the model, and produce a best-fit model that overpredicts the velocity dispersion at each of the four innermost points by \sim twice the measurement uncertainty in σ . We take $3000M_\odot$ as our upper limit on M_\bullet . This value is roughly ten times smaller than the value $\sim 5 \times 10^4 M_\odot$ inferred from ground-based data (4).

There is an empirical relation between the masses of SMBHs and the properties of their host bulges called the “ $M_\bullet - \sigma$ relation,” which is expressed as (14)

$$\frac{M_\bullet}{10^8 M_\odot} \approx 1.3 \left(\frac{\sigma_c}{200 \text{ km s}^{-1}} \right)^\alpha \quad (3)$$

with $\alpha = 4.80 \pm 0.54$. Here σ_c is the stellar velocity dispersion measured within an aperture of radius $r_e/8$ centered on the nucleus and r_e is the projected radius containing 1/2 of the light of the bulge. Because r_e is not well measured for the M33 bulge (estimates range from 0.5 kpc (2) to 2 kpc (10)), and the dependence of σ on radius is not known accurately outside of the central ~ 1 pc, we conservatively adopt $21 \text{ km s}^{-1} \leq \sigma_c \leq 34 \text{ km s}^{-1}$, the range of values measured between $0''$ and $80''$ (13). The $M_\bullet - \sigma$ relation then predicts a mass in the range $2600 \leq M_\bullet/M_\odot \leq 26300$, consistent with our upper limit. In contrast, the shallower $M_\bullet - \sigma$ relation proposed by Gebhardt et al. (15) would imply $M_\bullet \gtrsim 2.5 \times 10^4 M_\odot$, which is not consistent with the upper limit on M_\bullet obtained here.

The $M_\bullet - \sigma$ relation is used to study SMBH demographics and constrain models of black hole formation and evolution (16,17,18). The low-mass end of the relation is of particular importance because SMBHs larger than $\sim 10^6 M_\odot$ are believed to originate through physical processes different from those regulating the formation of smaller mass black holes (19,20). However, all supermassive black holes detected so far have masses $M_\bullet > 10^6 M_\odot$ (Fig 4). Evidence for “intermediate-mass black holes” (IMBHs), with masses in the range $10^2 M_\odot \lesssim M_\bullet \lesssim 10^5 M_\odot$, is so far only circumstantial and relies on speculations concerning the nature of the super-luminous off-nuclear X-ray sources (ULXs) detected in a number of starburst galaxies (21,22). The connections between the possible black hole in M33 and ULXs is tantalizing: the M33 nucleus itself contains the brightest ULX in the Local Group (23), and has optical and near-infrared colors and spectra consistent with those of a young cluster (3) with size and mass similar to those measured for the cluster containing the brightest of the M82 ULXs (5,24). However, because our upper limit on M_\bullet in M33 is consistent with the $M_\bullet - \sigma$ relation as defined by much brighter galaxies, we cannot yet conclude that the presence of a black hole in M33 would require a different formation mechanism from that of the SMBHs detected in other galaxies.

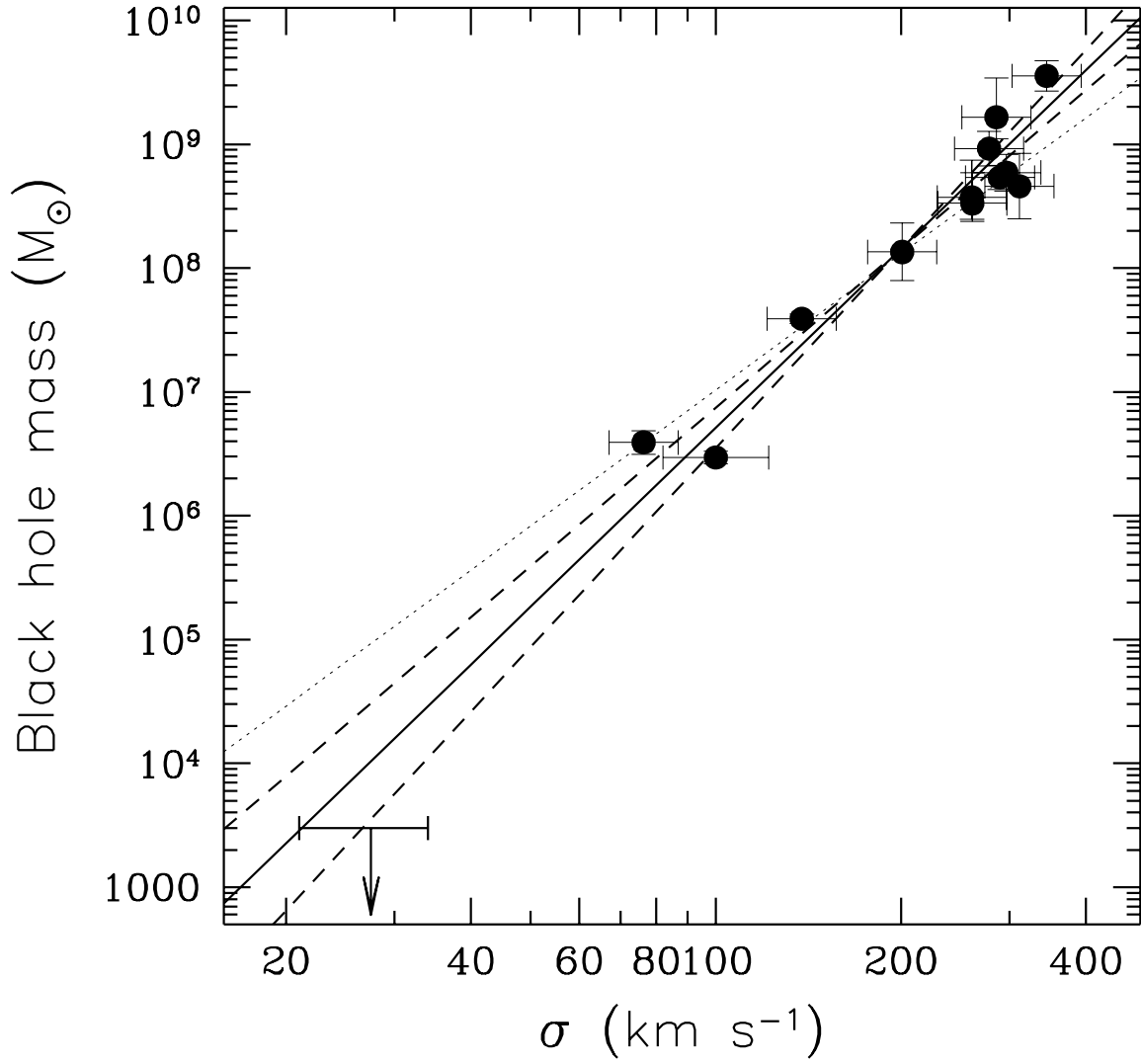


Figure 4. The thick solid line represents the $M_{\bullet} - \sigma$ relation as derived by Ferrarese & Merritt (14), with $1-\sigma$ confidence limits on the slope shown by the dashed lines. The upper limit for the black hole mass in M33 (shown by the arrow) is consistent with this relation but inconsistent with the shallower relation advocated by Gebhardt et al. (15) and shown by the thin dotted line.

References

1. van den Bergh, S. The local group of galaxies. *Ann. Rev. astron. Ap.* **9**, 273–318 (1999).
2. Minniti, D., Olszewski, E. W. & Rieke, M. The Bulge of M33. *Astrophys. J.* **410**, L79–L82 (1993).
3. van den Bergh, S. The stellar populations of M33. *Publ. Astron. Soc. Pacif.* **103**, 609–622 (1991).
4. Kormendy, J., & McClure, R. D. The nucleus of M33 *Astron. J.* **105**, 1793–1812 (1993).
5. Lauer, T. R., Faber, S. M., Ajhar, E. A., Grillmair, C. J. & Scowen, P. A., M32±1. *Astron. J.* **116**, 2263–2286 (1998).
6. van der Marel, R. The black hole mass distribution in early-type galaxies: cusps in Hubble Space Telescope photometry interpreted through adiabatic Black Hole growth. *Astron. J.* **117**, 744–763 (1999).
7. Joseph, C., et al. The nuclear dynamics of M32. I. Data and stellar kinematics. *Astrophys. J.* **550**, 668–690 (2001)
8. Merritt, D. Recovering velocity distributions via penalized likelihood. *Astron. J.* **114**, 228–237 (1997).
9. van der Marel, R. P., & Franx, M. A new method for the identification of non-Gaussian line profiles in elliptical galaxies. *Astrophys. J.* **407**, 525–539 (1993).
10. Regan, M. W., & Vogel, S. N. The near-infrared structure of M33. *Astron. J.* **434**, 536–545 (1994).
11. Takamiya, T., Sofue, Y. Radial distribution of the mass-to-luminosity ratio in spiral galaxies and massive dark cores. *Astrophys. J.* **534**, 670–683 (2000)
12. Merritt, D. Dynamical mapping of hot stellar systems. *Astrophys. J.* **413**, 79–94 (1993).
13. Minniti, D. Velocities of supergiants in the bulge of M 33. *Astron. Astrophys.* **306**, 715–720 (1996).
14. Ferrarese, L., & Merritt, D. A fundamental relation between supermassive black holes and their host galaxies. *Astrophys. J.* **539**, L9–L12 (2000).
15. Gebhardt, K. Bender, R., Bower, G., Dressler, A., Faber, S. M., Filippenko, A. V., Green, R., Grillmair, C., Ho, L. C., Kormendy, J., Lauer, T. R., Magorrian, J., Pinkney, J., Richstone, D., Tremaine, S. A relationship between nuclear black hole mass and galaxy velocity dispersion. *Astrophys. J.* **539**, L13–L16 (2000).
16. Haehnelt, M. G., & Kauffmann, G. The correlation between black hole mass and bulge velocity dispersion in hierarchical galaxy formation models. *Mon. Not. R. astron. Soc.* **318**, L35–L38 (2000).
17. Ciotti, L., & van Albada, T. S. The $M_{\bullet} - \sigma$ relation as a constraint on the formation of elliptical galaxies. Accepted by *Astrophys. J.* (astro-ph/0103336) (2001)

18. Merritt, D., & Ferrarese, L. Black Hole demographics from the $M_{\bullet} - \sigma$ relation. *Mon. Not. R. astron. Soc.* **320**, L30–L34 (2001).
19. Haehnelt, M. G., Natarajan, P., & Rees, M. J. The distribution of supermassive black holes in the nuclei of nearby galaxies. *Mon. Not. R. astron. Soc.* **308**, 77–81 (1998).
20. Miller, M. C., & Hamilton, D. P. Production of intermediate-mass black holes in globular clusters. Submitted to *Mon. Not. R. astron. Soc.* (astro-ph/0106188) (2001).
21. Matsumoto, H., Tsuru, T. G., Koyama, K., Awaki, H., Canizares, C. R.; Kawai, N., Matsushita, S., Kawabe, R. Discovery of a luminous, variable, off-center source in the nucleus of M82 with the Chandra High-Resolution Camera. *Astrophys. J.* **547**, L25–L28 (2001)
22. Fabbiano, G., Zezas, A., Murray, S.S. Chandra observations of “the Antennae” galaxies (NGC 4038/39). Accepted by *Astrophys. J.* (astro-ph/0102256) (2001)
23. Long, K.S., Dodorico, S., Charles, P.A., & Dopita, M.A. Observations of the X-ray sources in the nearby SC galaxy M33. *Astrophys. J.* **246**, L61–L64 (1981)
24. Ebisuzaki, T., Makino, J., Tsuru, T. G., Funato, Y., Portegies Zwart, S., Hut, P., McMillan, S., Matsushita, S., Matsumoto, H., & Kawabe, R. Missing link found? — the “runaway” path to supermassive black holes. Submitted to *Astrophys. J.* (astro-ph/0106252) (2001).
25. This work was supported by the National Science Foundation through grant 4-21911, and by the National Aeronautics and Space Administration through grants 4-21904 and NAG5-8693.